Yielding and Flow of Soft-Jammed Systems in Elongation

X. Zhang, Omar Abdoulaye Fadoul, Elise Lorenceau, Philippe Coussot

Editors' Suggestion

Yielding and Flow of Soft-Jammed Systems in Elongation

X. Zhang,[1] O. Fadoul,[1] E. Lorenceau,[2] and P. Coussot[1]

[1] *Université Paris-Est, Laboratoire Navier (ENPC-IFSTTAR-CNRS), 2 Allée Kepler, 77420 Champs sur Marne, France*

[2] *Université Grenoble Alpes, CNRS, LIPhy, 38000 Grenoble, France*

(Received 10 September 2017)

So far, yielding and flow properties of soft-jammed systems have only been studied from simple shear and then extrapolated to other flow situations. In particular, simple flows such as elongations have barely been investigated experimentally or only in a nonconstant, partial volume of material. We show that using smooth tool surfaces makes it possible to obtain a prolonged elongational flow over a large range of aspect ratios in the whole volume of material. The normal force measured for various soft-jammed systems with different microstructures shows that the ratio of the elongation yield stress to the shear yield stress is larger (by a factor of around 1.5) than expected from the standard theory which assumes that the stress tensor is a function of the second invariant of the strain rate tensor. This suggests that the constitutive tensor of the materials cannot be determined solely from macroscopic shear measurements.

DOI:

The concept of jamming to characterize materials has flourished and appeared quite useful. Soft-jammed systems, such as foams, emulsions, concentrated suspensions, and colloids, have a structure in which the elements are trapped in potential wells due to their interactions (varying with the distance) with their neighbors and cannot move out due to thermal agitation alone [1]. It is necessary to apply a stress larger than a critical value, i.e., the yield stress (τ_c), to break the structure and induce a flow of the system, otherwise, they behave as solids [1,2].

This concept and its experimental validation, nevertheless, essentially went through simple shear experiments, i.e., a situation where the structure breaks via a relative gliding of material layers along a planar direction. In that case (simple shear), the behavior of granular materials [3], simple yield stress fluids [4], or more complex systems with a behavior depending on the flow history (aging) [5] have been well characterized. However, in many real flow conditions, such as extrusion, blade coating, squeezing, extension, etc., the flow is more complex as it involves some elongational component. In that case, the material undergoes a shrinkage in one direction while being extended in a perpendicular direction. How the yielding properties under such conditions are related to the yield stress observed in simple shear or, more generally, to the material structure, constitutes an open question.

The description of complex flows requires a 3D expression of the constitutive equation. So far, for soft-jammed systems, it has been considered that the stress tensor (**T**) is proportional to the strain rate tensor (**D**) as for Newtonian fluids but with a factor of proportionality (i.e., the apparent viscosity) depending nonlinearly on the flow intensity. For sufficiently slow flows, i.e., for which the rate-dependent term of the constitutive equation is negligible, this factor is $\tau_c/\sqrt{-D_{\mathrm{II}}}$ where D_{II} is the second invariant of **D** ($D_{\mathrm{II}} = -\mathrm{tr}\mathbf{D}^2/2$ for an incompressible material), whatever the flow type [6]. This approach has the advantage of predicting the correct yield stress value for simple shear or more complex shear flows [7] and to be consistent with the usual description of the yielding behavior of some solid materials. It is at the basis of models used for the complete numerical simulations of complex yield stress fluid flows [8] but also of granular flows [9]. For a simple uniaxial elongation, this approach predicts that the yielding and slow flow should occur for a normal stress difference (σ) equal to $\sqrt{3}\tau_c$ [10].

In fact, it is not clear at all that soft-jammed systems should follow such a simple 3D behavior. Indeed, the physical origin of this homogeneous 3D constitutive equation for a simple fluid is that all the elements (i.e., molecules) rapidly explore various positions and, thus, can reach the most appropriate ones under some stress. As soon as some significant structural aspect—such as collective arrangement, deformation, or orientation of the elementary components of the fluid—is introduced in a system, it might behave differently, as suggested in Ref. [11]. For example, for polymers whose orientation and length can vary with the flow characteristics, the elongational viscosity may be several orders of magnitude larger than the shear viscosity, whereas the basic linear 3D expression predicts a ratio of 3 [12]. Thus, we can wonder if this homogeneous behavior is still valid for jammed systems in which the structure plays a major role and/or what the relation is between σ and τ_c. Actually, experimental data on such a flow type are scarce, and the conclusions remain fragile because in these experiments, the (supposedly) elongated region was confined in a specific (small) volume of the sample which continuously evolved during the test [13].

Finally, contradictory results were obtained, σ being found between $\sqrt{3}\tau_c$ and $3\sqrt{3}\tau_c$ [13–17].

Here we propose an original approach which makes it possible to get a prolonged elongational flow over a large range of aspect ratios in the whole volume of material. This is obtained by considerably reducing the shear stress along the walls by using smooth surfaces. Data for σ obtained for different soft-jammed systems are significantly larger than expected from the standard theory, which suggests that the yielding and flow properties of jammed systems are more complex than assumed so far.

An approach standard for polymers [18] to obtain an elongational flow consists to move away two plates in contact with a cylindrical layer of a soft-jammed system (of volume Ω and initial thickness h_0) at a velocity $U = dh/dt$, where h is the current distance between the plates. As h increases, it is expected that the sample will approximately keep a cylindrical shape, while its aspect ratio, i.e., h/R, where R is the current radius of the (cylindrical) sample, increases. Such a situation corresponds to a simple uniaxial elongation. However, for soft-jammed systems and sufficiently slow flows, when the initial aspect ratio is large (say, $h_0/R_0 \gg 0.1$), the sample immediately evolves as two conical parts which eventually separate [19,20]. This effect results from the intrinsic yielding behavior of the material and the boundary conditions. Since the line of contact is pinned, an increase of h induces a reduction of the sample diameter in the central region. Since the (traction) force (F) is transmitted vertically through the sample, the (mean) normal stress is larger for a smaller sample diameter. Then the stress may be larger than σ at some distance from the plates, while it remains smaller elsewhere. This effect leads to the stoppage of a growing material volume along each plate while the flow goes on concentrating in the central region, which finally leads to the formation and separation of two (approximately) conical shapes.

To damp this effect, we can start from a much smaller separating distance than the cylinder radius, i.e., $h_0/R_0 \ll 1$, since then the relative stress difference in different sample layers will be smaller. However, in that case, the radial fluid velocity towards the center V is much larger than U, since due to sample volume conservation ($\Omega = \pi R^2 h$): $V = -dR/dt = (R/2h)U$. This induces a significant shear flow before the fluid separates in two parts, and finally, F is essentially due to the radial gradient of pressure induced by this lubricational flow. For slow flows, F is now proportional to τ_c and scales with $h^{-2.5}$ [10,21]. In fact, under such conditions, the peripheral interface is unstable and fingering generally occurs [20,22]. This leads to a force smaller than predicted by this theory [20] yet with F still approximately scaling with $h^{-2.5}$ (see Fig. 1). Nevertheless, when h_0/R_0 is increased, F increases and, in a regime intermediate between well-developed fingering and direct separation in two cones, we finally get a force curve close to the theoretical prediction (see Fig. 1). This anyway does not correspond to an elongational flow.

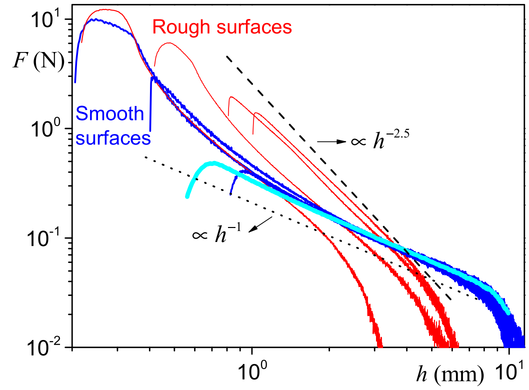

FIG. 1. Force vs distance during a traction experiment for a direct emulsion (82%) with rough plates (thin red curves) or smooth surfaces (thick dark blue curves) for different initial aspect ratios (corresponding to first point of curves on the left) at $U = 0.01$ mm/s ($\Omega = 3$ ml). The very thick light blue line corresponds to $U/h = \mathrm{const} = 0.01\ \mathrm{s}^{-1}$. The dashed line is the lubrication model (see text), and the dotted line is the standard theoretical curve for slow elongation.

In the above situations, the fluid adherence on the solid plate surface is at the origin of the deviation of the flow from a simple elongation. In order to suppress or at least strongly reduce this adherence, we can use two smooth silicon surfaces, along which it is known that due to a wall slip effect [23,24], the tangential flow of a soft-jammed system is greatly facilitated: the material can move as a solid block for a shear stress much smaller than τ_c. Under such conditions, we observe that the material keeps a cylindrical shape all along the process, with a slight evolution of the curvature of the peripheral-free surface (see Fig. 2), and this (approximate) cylinder progressively stretches. The simplest velocity field compatible with the mass conservation and this evolution of the boundaries (neglecting the curvature) over more than a decade of h expresses as follows in cylindrical coordinates: $v_r = -r\dot{\varepsilon}/2$, $v_\theta = 0$, $v_z = z\dot{\varepsilon}$, with $\dot{\varepsilon} = (dh/dt)/h = U/h$ the strain rate. This corresponds to a simple uniaxial elongational flow.

Let us now look at the variations of the force $F(h)$ needed to impose this flow (see Fig. 1). First, it increases from a low value, as the material is essentially deformed in its solid regime, then it starts to decrease, first rapidly, then more slowly and finally follows a decrease as $1/h$ over a significant range of h, i.e., 1.5–7 mm. For the analysis below, we will not consider the ultimate flow stage at larger h, where the force drops to zero (see Ref. [10]).

Interestingly, the force decrease does not depend on h_0 (see Fig. 1). This differs from flows with rough surfaces for which there is an increasing volume of arrested material, leading to different force curves for different initial distances (see Fig. 1). This suggests that the material deformation follows the same path in any case (starting from

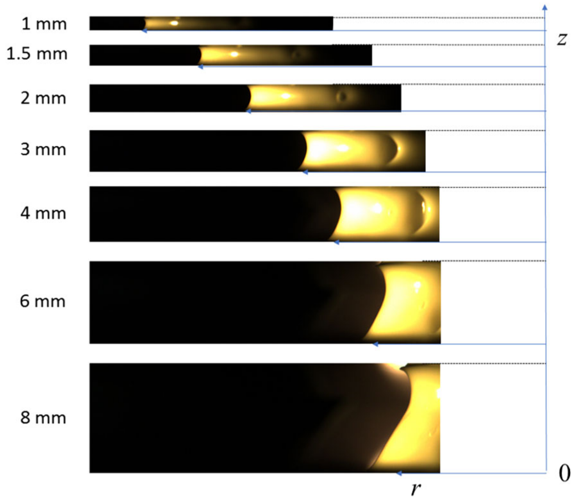

FIG. 2. Successive views for different plate distances during relative motion of two plates in contact via an emulsion (82%) (yellow region). Here, only one side (relative to the axis) is (partially) shown (the zones between the yellow regions and the vertical axis are, in fact, filled with material), the central axis is shown in blue on the right, and the mean sample radius is represented by horizontal arrows.

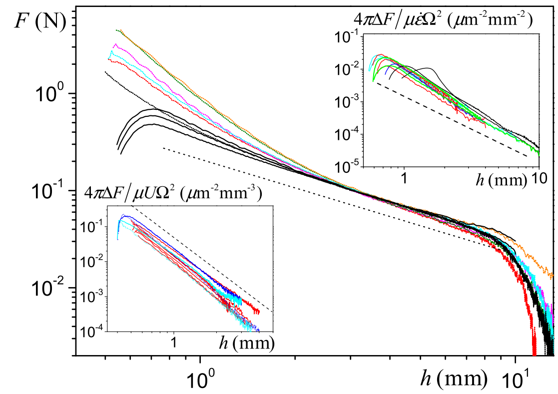

FIG. 3. Force vs height curve with smooth surfaces during traction on a yield stress fluid (emulsion 82%) for $\Omega = 3$ ml and different U [(dotted lines) from bottom to top, 0.01, 0.02, 0.03, 0.05, 0.07, 0.1 $\mathrm{mm\,s^{-1}}$] or $\dot{\varepsilon}$ [(continuous curves) from bottom to top, 0.01, 0.02, 0.03 $\mathrm{s^{-1}}$]. The straight dotted line is the standard expression for normal force in elongation. The lower inset shows the rescaled residual force (see text) as a function of the distance for the above data (red) at constant U and for data obtained with emulsions at 76% (light blue) and 85% (dark blue) at $U = 0.01$ and $0.05\ \mathrm{mm\,s^{-1}}$. The dashed line has a slope of -3 in logarithmic scale. The higher inset shows the rescaled residual force for data of the main graph (red) at constant $\dot{\varepsilon}$ and for emulsions at 76% (light blue) and 85% (dark blue) at 0.01 and 0.04 $\mathrm{s^{-1}}$, and 82% with a glycerol solution (black) at $\dot{\varepsilon} = 0.01$ and 0.04 $\mathrm{s^{-1}}$. Data for an emulsion with smaller droplet size (i.e., 0.7 μm) at $\dot{\varepsilon} = 0.01$ and 0.04 $\mathrm{s^{-1}}$ are also shown (green). The dotted line has a slope -2 in logarithmic scale. No particular tendency of variation as a function of U or $\dot{\varepsilon}$ may be observed in the inset graphs.

different points) and confirms that all the sample volume is involved in the same flow type at any time.

We can also remark that F is initially smaller when U is decreased and reaches the region $F \propto 1/h$ sooner where all curves tend to superimpose (see Fig. 3). Thus, we can define a factor α such that all force curves are situated above α/h and, for a given h, tend to this value when $U \to 0$. We also performed tests by decreasing U when h decreases (i.e., $U \propto h$), which allows us to reach this asymptotic curve for even lower h (see Fig. 3). This has the advantage of corresponding to a constant strain rate $\dot{\varepsilon} = U/h$, which means that we impose a constant dynamics of elongation to the material. In that case, we also observe (see Fig. 3) that the asymptotic curve is reached more rapidly for lower $\dot{\varepsilon}$. We conclude that the minimum force curve that may be reached for slow flows is $F \propto \alpha/h$, where α is a factor depending on the sample volume and material characteristics. This situation is rapidly reached for low $\dot{\varepsilon}$ (typically, 0.01 $\mathrm{s^{-1}}$) so that F follows this law over one decade of h (i.e., here in the range 0.7–7 mm) (see Figs. 3 and 4), which corresponds to a range of aspect ratios varying over one and a half decades [since $h/R = h/(\Omega/\pi h)^{1/2} \propto h^{1.5}$]. Moreover, it may be shown that surface tension and gravity effects can be neglected (see Ref. [10]), which means that the normal force recorded essentially corresponds to viscous effects in the bulk.

The deviation of F from α/h observed at a small h and more pronounced for large U is somewhat intriguing. It might be due to the rate-dependent term in the constitutive equation becoming significant at large $\dot{\varepsilon}$. However, we observe that this effect occurs even under constant $\dot{\varepsilon}$ (see Fig. 3). Moreover, an estimation of the rate-dependent term shows that for an elongation, it is always much smaller than the (constant) plastic term, typically by a factor less than 5% [10]. Such a value is very low in regard to the observed deviation, which reaches about 300% in some cases (see Fig. 3). We conclude that in our tests, U should not have a significant impact on $F(h)$ as long as the flow effectively corresponds to a uniaxial elongation. Necessarily, the observed deviation from α/h results from a slightly more complex flow; for example, in the regions of largest relative velocity between the material and the solid surfaces, i.e., at the periphery, some shearing might occur, even if most of the sample volume still undergoes a pure elongational flow. These observations, nevertheless, provide information about the wall slip process in that case.

Indeed, let us consider that all occurs as if there were layers of the interstitial liquid of the material of thickness δ and viscosity μ situated between the bulk and the solid surfaces. These liquid layers essentially allow us to strongly reduce the (shear) adherence of the material to the solid surface, but they also transmit the normal force needed to induce the bulk flow. Since $\delta \ll R$, these layers undergo a (lubricational) shear flow due to the relative motion of their boundaries: the solid surface on one side and the interface

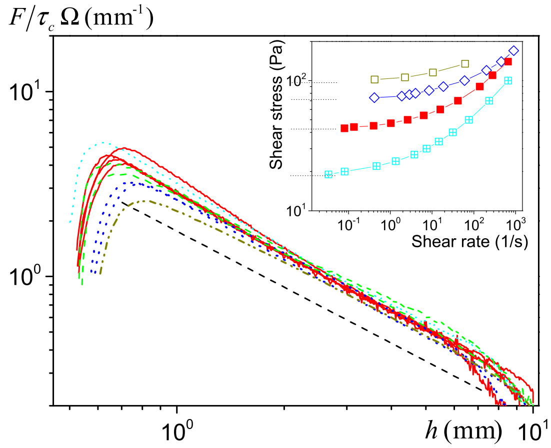

FIG. 4. Rescaled force vs height during traction tests at a constant strain rate (0.01 s^{-1}) for emulsions at a concentration of 82% for different volumes (1, 2, 3, and 4 ml) (continuous red curves); emulsions at concentrations 76% (dotted light blue) (3 ml), 85% (dotted dark blue) (1 and 3 ml), and 87% (brown dash dotted line) for 3 ml; a Carbopol gel (dashed green) for 1 and 3 ml. The dotted straight line corresponds to $\sigma = \sqrt{3}\tau_c$. Reproducibility tests show that the uncertainty on these data is 10% (see Ref. [10]). The inset shows the flow curves in simple shear for the three emulsions (from bottom to top) 76%, 82%, 85%, 87%. The dotted lines show the level of yield stress as deduced from creep tests. The uncertainty on these values is less than 5% (see Ref. [10]).

with the shrinking bulk on the other side. The resulting normal force from the induced pressure gradient writes $F = -p_R\Omega/h + \mu\Omega^2 U/4\pi h^3\delta^2$. The pressure term p_R (negative, relative to the ambient pressure) *a priori* results from the Laplace pressure drop associated with the curvature of the liquid-air interface. The validity of this expression may be checked on our data by withdrawing from each experimental force curve a $-p_R\Omega/h$ term fitted to the data at large h values (i.e., when the second term is negligible). The residual force (i.e., $\Delta F = F + p_R\Omega/h$) effectively varies as a function of h, Ω, μ, and U as predicted by the above expression, i.e., $4\pi\Delta F/\mu\Omega^2 U = 1/h^3\delta^2$ for constant U and $4\pi\Delta F/\mu\Omega^2\dot{\varepsilon} = 1/h^2\delta^2$ for constant $\dot{\varepsilon}$ (see the insets of Fig. 3). The value for δ may, thus, be deduced from the comparison of the data with the theoretical expression.

From this analysis, we surprisingly find a constant value for the wall slip layer thickness under any conditions in our range of tests (see the insets of Fig. 3): $\delta = 9 \pm 3$ μm. This means that the liquid volume available for slip continuously adjusts during traction, an effect likely due to the reentrance of the liquid in the material structure as it shrinks. Note that this reentrance, which could affect the flow characteristics and, thus, modify the second term of the force expression, has apparently a negligible impact. Another surprising result is that δ is several orders of magnitude larger than in simple shear for the same kinds of material (i.e., 35 ± 15 nm; see Ref. [24]) but with no clear relation with a characteristic length of the material structure (here droplet size) (see the top inset of Fig. 3). This suggests that wall slip in an elongational process has a different nature than in simple shear.

Let us come back to the $1/h$ regime for the bulk flow. We can now compute a normal stress $\sigma = F/\pi R^2$, which, due to mass conservation, may also be expressed as Fh/Ω. Our results show that at sufficiently low $\dot{\varepsilon}$, σ is a constant equal to $\sigma = \alpha/\Omega$. Further tests (see Fig. 4) show that α is proportional to Ω, which means that σ is independent of Ω. Finally, these tests allow us to measure a quantity, i.e., the normal stress σ, which is independent of the current aspect ratio and the size of the material, as long as the sample remains cylindrical. This is the *normal stress difference* associated with a simple uniaxial elongation flow at sufficiently low $\dot{\varepsilon}$ (see Ref. [10]), which here appears to be an intrinsic property of the soft-jammed system. Since this value is the minimal normal stress that must be applied to impose such an elongational flow, this is the (simple uniaxial) elongation yield stress.

Note that in contrast with usual approaches which studied elongational flows in a localized volume of the sample during a transient flow [13–17], here we have *a priori* a straightforward measure of the normal stress needed to impose a prolonged elongational flow in the whole sample volume and over a significant range of aspect ratios.

In addition, we independently determined the (shear) yield stress for our different materials from a well-controlled series of precise creep tests in shear geometry which allow us to clearly distinguish the liquid and the solid regimes and the critical stress (τ_c) associated with the transition. These data also provide the simple shear flow curve (see the inset of Fig. 4), whose validity was checked through tests with other procedures and equipment (see Ref. [24]). Further traction tests then show that for a given material type, σ is simply proportional to τ_c (see Fig. 4). The factor of proportionality is equal to $1.5\sqrt{3}$ for emulsions and Carbopol gels at various concentrations (see Fig. 4), which is 1.5 larger than predicted by the standard theory. This factor is even larger for two more complex materials (mustard and ketchup), i.e., of the order of $2.5\sqrt{3}$ (see Ref. [10]). These results show that the assumption of a factor depending only on the second invariant in the constitutive equation, and, thus, being equal to $\sqrt{3}$, is not valid. A possibility is that the parameters of this constitutive equation depend on the third invariant of $\mathbf{D}$ [i.e., $D_{III} = \det(\mathbf{D})$], as suggested in Ref. [15], e.g., with now the extrastress tensor expressing as $\tau_c\mathbf{D}/[(-D_{II})^{1/2} + \alpha D_{III}{}^{1/3}]$ in slow flows. For the emulsions and Carbopol gels, $\alpha = -0.46$ allows us to well represent the data. One may also think of using other plasticity criteria for expressing this first term of the constitutive equation.

This shows that the standard simple view of jamming described with a homogeneous approach (i.e., second invariant of the stress tensor) is not valid. Our results suggest that the 3D expression of their constitutive equation is more complex than suggested so far and cannot leave apart the specificities of the material structure, and more particularly, the physical origin of jamming, e.g., squeezed objects or particles interacting at a distance. This also implies that appropriate models of the constitutive equation, in particular, for yielding and slow flow regime, have to be developed.

This work has benefited from a French government grant managed by ANR within the frame of the national program Investments for the Future ANR-11-LABX-022-01.

[1] A. J. Liu and S. R. Nagel, Nature (London) **396**, 21 (1998).
[2] P. Coussot, *Rheometry of Pastes, Suspensions and Granular Materials* (Wiley, New York, 2005).
[3] G. D. R. Midi, Eur. Phys. J. E **14**, 341 (2004).
[4] G. Ovarlez, S. Cohen-Addad, K. Krishan, J. Goyon, and P. Coussot, J. Non-Newtonian Fluid Mech. **193**, 68 (2013).
[5] G. Ovarlez, S. Rodts, X. Chateau, and P. Coussot, Rheol. Acta **48**, 831 (2009).
[6] J. G. Oldroyd, Proc. Cambridge Philos. Soc. **43**, 100 (1947); J. M. Piau, Tech. Ing. A **710**, A711 (1979).
[7] G. Ovarlez, Q. Barral, and P. Coussot, Nat. Mater. **9**, 115 (2010).
[8] P. Saramito and A. Wachs, Rheol. Acta **56**, 211 (2017).
[9] P. Jop, Y. Forterre, and O. Pouliquen, Nature (London) **441**, 727 (2006).
[10] See the Supplemental Material at http://link.aps.org/supplemental/10.1103/PhysRevLett.000.000000, which includes information about the surface characteristics, rheometry, basic theory, procedure for the elongation tests, reproducibility, additional data, lubricational flow, flow in the slip layer, surface tension effects, gravity effects, and the relative importance of the different stress terms.
[11] J. M. Brader, M. E. Cates, and M. Fuchs, Phys. Rev. Lett. **101**, 138301 (2008).
[12] C. W. Macosko, *Rheology Principles, Measurements and Application* (VCH, New York, 1994).
[13] J. Boujlel and P. Coussot, Soft Matter **9**, 5898 (2013).
[14] G. German and V. Bertola, Phys. Fluids **22**, 033101 (2010).
[15] K. Niedzwiedz, H. Buggisch, and N. Willenbacher, Rheol. Acta **49**, 1103 (2010); L. Martinie, H. Buggisch, and N. Willenbacher, J. Rheol. **57**, 627 (2013).
[16] N. Louvet, D. Bonn, and H. Kellay, Phys. Rev. Lett. **113**, 218302 (2014).
[17] M. K. Tiwari, A. V. Bazilevsky, A. L. Yarin, and C. M. Megaridis, Rheol. Acta **48**, 597 (2009).
[18] G. H. McKinley and T. Sridhar, Annu. Rev. Fluid Mech. **34**, 375 (2002).
[19] P. Coussot and F. Gaulard, Phys. Rev. E **72**, 031409 (2005); N. J. Balmforth, N. Dubash, and A. C. Slim, J. Non-Newtonian Fluid Mech. **165**, 1147 (2010).
[20] Q. Barral, G. Ovarlez, X. Chateau, J. Boujlel, B. Rabideau, and P. Coussot, Soft Matter **6**, 1343 (2010).
[21] G. H. Covey and B. R. Stanmore, J. Non-Newtonian Fluid Mech. **8**, 249 (1981); G. H. Meeten, Rheol. Acta **41**, 557 (2002).
[22] D. Derks, A. Lindner, C. Creton, and D. Bonn, J. Appl. Phys. **93**, 1557 (2003).
[23] M. Cloitre and R. T. Bonnecaze, Rheol. Acta **56**, 283 (2017).
[24] X. Zhang, E. Lorenceau, P. Basset, T. Bourouina, F. Rouyer, J. Goyon, and P. Coussot, Phys. Rev. Lett. **119**, 208004 (2017).